AUTOMATIC SENSOR ORIENTATION REFINEMENT OF PLÉIADES STEREO IMAGES

C. de Franchis[⋆] *E. Meinhardt-Llopis*[⋆] *J. Michel*[†] *J.-M. Morel*[⋆] *G. Facciolo*[⋆]

[⋆] Ecole normale supérieure de Cachan, Centre de mathématiques et de leurs applications
61 Avenue du Président Wilson, 94230 Cachan, France
[†] CNES - DCT/SI/AP
18 Avenue Edouard Belin, 31401 Toulouse, France

ABSTRACT

Modern Earth observation satellites are calibrated in such a way that a point on the ground can be located with an error of just a few pixels in the image domain. For many applications this error can be ignored, but this is not the case for stereo reconstruction, that requires sub-pixel accuracy. In this article we propose a method to correct this error. The method works by estimating local corrections that compensate the error relative to a reference image. The proposed method does not rely on ground control points, but only on the relative consistency of the image contents. We validate our method with Pléiades and WorldView-1 images on a representative set of geographic sites.

1. INTRODUCTION

The Pléiades constellation is composed of two twin Earth observation satellites operating in the same orbit and phased $180°$ apart. Both are high resolution satellites, able to deliver images with a ground sampling distance of 70 cm and a swath width of 20 km. The images have a pixel depth of 12 bits with a signal-to-noise ratio greater than 90 dB.

The unique agility of the Pléiades satellites allows them to capture multiple views of the same target in a single pass. This permits nearly simultaneous stereo or tri-stereo acquisitions with a small base to height ratio (B/H), ranging from 0.15 to 0.8. Stereo and tri-stereo datasets are aimed at producing accurate 3D models. The internal and external parameters of the pushbroom camera system are known, including the effects of the atmospheric refraction. Thus, each image is accompanied by a pair of functions that describe the formation model. These functions permit a conversion of image coordinates to globe coordinates, and back.

There is a noticeable error of a few pixels on these functions [1, 2, 3, 4]. For many purposes this error can be ignored since it typically results in a global offset of the results. However, for stereo applications, the epipolar constraints derived from the parameters of the cameras have to be as precise as possible. This work proposes a method to correct this error relative to a given reference image. Our method does not rely on ground control points, but on the relative consistency of the image contents. It can thus be implemented as an automatic pre-processing of the input images.

1.1. The rational polynomial camera model

An image is obtained by projecting 3-space points on a plane with a function $\mathbf{R}^3 \to \mathbf{R}^2$, $(\varphi, \lambda, h) \mapsto (x, y)$, where 3-space points are represented by their spheroidal coordinates in the World Geodetic System (WGS 84). In that system a point of 3-space is identified by its latitude $\varphi \in]-90, 90[$, longitude $\lambda \in]-180, 180]$ and its altitude h, in meters, above the reference ellipsoid. This *projection function* depends only on the position of the camera with respect to the coordinate system. The *localization function* $\mathbf{R}^3 \to \mathbf{R}^3$, $(x, y, h) \mapsto (\varphi, \lambda, h)$ is its inverse with respect to the first two components. It takes a point $\mathbf{x} = (x, y)$ in the image together with an altitude h, and returns the coordinates of the corresponding 3-space point $\mathbf{X} = (\varphi, \lambda, h)$.

The *Rational Polynomial Coefficient* (RPC) camera model is an analytic description of the projection and localization functions. These functions are expressed as ratio of multivariate cubic polynomials [5, 6, 7]. For the sake of clarity, we shall denote by $\text{RPC}_u : \mathbf{R}^3 \to \mathbf{R}^2$ the projection function of the RPC model associated to image u, and by $\text{RPC}_u^{-1} : \mathbf{R}^3 \to \mathbf{R}^3$ the corresponding localization function.

2. THE RELATIVE POINTING ERROR

2.1. Epipolar curves

The knowledge of the projection function RPC and the associated inverse RPC^{-1} for two images u and v allows to define epipolar curves. If $\mathbf{x}$ is a point in image u, then the function

$$\text{epi}_{uv}^{\mathbf{x}} : h \longmapsto \text{RPC}_v(\text{RPC}_u^{-1}(\mathbf{x}, h))$$

defines a parametrized curve in the domain of image v containing all the possible correspondences of $\mathbf{x}$ for different altitudes h. This curve is called the *epipolar curve* of the point $\mathbf{x}$. In practice, we observe that these curves are locally straight line segments which are almost parallel (see Figure 1).

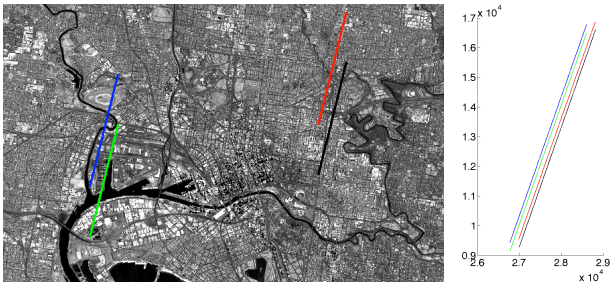

Fig. 1. The RPC functions allow to draw the epipolar curves for a pair of Pléiades images u and v (approx. $40\,000 \times 16\,000$ pixels). The left image shows four epipolar curves plotted in the domain of image v. They correspond to four points located near the edges of the image u. The range of altitudes considered is $h \in [-200, 3000]$ meters. The right image shows the same epipolar curves placed closer to facilitate the comparison.

The epipolar curves are useful to compute the altitudes of points on the ground which are visible in two images. Suppose that $\mathbf{x}$ is the projection of a 3-space point in image u, and $\mathbf{x}'$ is the projection of the same point in image v. Then the epipolar curve of $\mathbf{x}$ passes through $\mathbf{x}'$ and the value h for which $\mathbf{x}' = \mathrm{epi}_{uv}^{\mathbf{x}}(h)$ is the altitude of the 3-space point.

2.2. Relative pointing error evidence

The RPC functions simplify the manipulation of the image formation model. However, due to inevitable errors in the estimation of the external parameters of the system, the formation model itself may not agree with the images. Given a pair of corresponding points $\mathbf{x}$ and $\mathbf{x}'$ in two images, the epipolar curve of $\mathbf{x}$ may not pass through the point $\mathbf{x}'$ (see Figure 2). We call this error the *relative pointing error*. It is not negligible at all, being often of the order of tens of pixels, as shown by Table 1.

2.3. How to measure the relative pointing error

Given two images u and v and a set of correspondences $(\mathbf{x}_i, \mathbf{x}'_i)_{i=1\ldots N}$, the relative pointing error between u and v is defined by

$$\frac{1}{N} \sum_{i=1}^{N} \mathrm{d}(\mathbf{x}'_i, \mathrm{epi}_{uv}^{\mathbf{x}_i}(\mathbf{R})). \qquad (1)$$

Here $\mathrm{epi}_{uv}^{\mathbf{x}_i}(\mathbf{R})$ is the epipolar curve of point $\mathbf{x}_i$, and d is the Euclidean distance between a point and a subset of $\mathbf{R}^2$. The set of correspondences between two images can be determined using SIFT [8]. Table 1 gives values for the relative pointing error measured on several Pléiades and Worldview-1 stereo pairs.

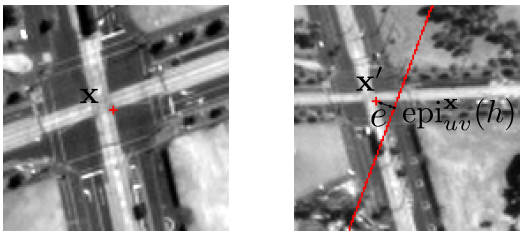

Fig. 2. This pair of Pléiades views of a road intersection evidences the effect of the satellite relative pointing error. Two corresponding points $\mathbf{x}$ and $\mathbf{x}'$ are shown but the epipolar curve of $\mathbf{x}$ as traced by the RPC doesn't pass through the corresponding point $\mathbf{x}'$. The *relative pointing error*, denoted by e, is the distance from the point $\mathbf{x}'$ to the epipolar curve $\mathrm{epi}_{uv}^{\mathbf{x}}(\mathbf{R})$. The altitude of the 3-space point corresponding to $\mathbf{x}$ and $\mathbf{x}'$ is approximated by the parameter h for which the epipolar curve passes through the projection of $\mathbf{x}'$.

3. CORRECTION OF THE RELATIVE POINTING ERROR

3.1. Not absolute but automatic correction

The error affecting RPCs is well known [2]. It is due to errors in the estimation of the sensor orientation, thus the approximation made by the RPC model is not to blame for it [4]. This error is absolute, which means that the image on u of ground control point with known geodetic coordinates $\mathbf{X}$ is not exactly located at the pixel predicted by $\mathrm{RPC}_u(\mathbf{X})$. Several authors have modeled this absolute error and proposed methods to compensate it [2, 4, 1, 3]. All these methods need GCPs and manual interactions, thus are not suitable in an automatic digital elevation model (DEM) generation procedure.

The relative pointing error is measured using two images and can be corrected without any control points. This correction will not remove the absolute error affecting the RPCs, but will allow to perform efficient stereo matching between the views by following epipolar curves. Moreover, this correction procedure does not require any manual interaction and can be integrated in a fully automatic DEM generation pipeline.

3.2. Relative pointing error model

As mentioned by Fraser and Hanley [4], errors within the direct measurement of sensor orientation reside mainly in sensor attitude. If we assume that the scene is located at infinity with respect to the satellite, an error in the sensor attitude measurement can be modeled in image space as a translation composed with a rotation. Thus the error can be corrected by transforming one of the two images, in such a way that the corresponding points fall on the respective epipolar curves. Let us assume that we have N correspondences $(\mathbf{x}_i, \mathbf{x}'_i)_{i=1,\ldots,N}$ between u and v, expressed in homogeneous coordinates. The problem is to estimate a translation $\mathtt{T}$ and

a rotation $\mathtt{R}$ centered in the center of the tile such that each transformed point $\mathtt{RT}\mathbf{x}'_i$ lies as close as possible to the epipolar curve $\mathrm{epi}^{\mathbf{x}_i}_{uv}(\mathbf{R})$. This could be done by minimizing the function

$$E_{uv}(\mathtt{R},\mathtt{T}) = \sum_{i=1}^{N} \mathrm{d}(\mathtt{RT}\mathbf{x}'_i, \mathrm{epi}^{\mathbf{x}_i}_{uv}(\mathbf{R})) + \lambda |h_i - h_i^0|^2, \quad (2)$$

where h_i (resp. h_i^0) is the altitude for which the epipolar curve $\mathrm{epi}^{\mathbf{x}_i}_{uv}(\mathbf{R}))$ passes through the projection of $\mathtt{RT}\mathbf{x}'_i$ (resp. $\mathbf{x}'_i$). The situation is illustrated on Figure 2.

The parameter λ was chosen empirically and fixed to 0.01. The first term measures the error in the direction perpendicular to the epipolar curve, while the second term penalizes the displacement along the epipolar line. A nonzero first term implies a violation of the epipolar constraint, thus the first term must be minimized. The second term is needed to prevent the solution from deriving towards an arbitrary large displacement along the epipolar curve. The weights reflect the relative importance of these two errors. Moreover, using a linear penalty for the first term and a quadratic one for the second leads to a soft constraint on the second term.

The goal of the relative pointing error correction is to improve the precision of the epipolar constraints derived from the RPC functions. Epipolar constraints are used to rectify the images for efficient stereo-matching. But as was previously shown [9], stereo-rectification of pushbroom images is possible only on small image tiles. For Pléiades images an appropriate tile size was found to be 1000×1000 pixels. On such small tiles the rotation component $\mathtt{R}$ of the pointing error is not visible. The function E_{uv} being minimized can thus be simplified and becomes:

$$E'_{uv}(\mathtt{T}) = \sum_{i=1}^{N} \mathrm{d}(\mathtt{T}\mathbf{x}'_i, \mathrm{epi}^{\mathbf{x}_i}_{uv}(\mathbf{R})). \quad (3)$$

3.3. Correction algorithm

Our study on stereo-rectification of pushbroom images [9] shows that the epipolar curve $\mathrm{epi}^{\mathbf{x}_i}_{uv}(\mathbf{R})$ is approximated up to 0.05 pixels by the line $\mathtt{F}\mathbf{x}_i$, where $\mathtt{F}$ is the affine fundamental matrix between the two views for the considered tile. As $\mathtt{F}$ is an *affine* fundamental matrix, all the lines $\mathtt{F}\mathbf{x}_i$ are parallel. Without any additional restriction, we may assume that these lines are horizontal. The horizontal line $\mathtt{F}\mathbf{x}_i$ can be written, in homogeneous coordinates, as

$$\mathtt{F}\mathbf{x}_i = \begin{bmatrix} 0 \\ 1 \\ c_i \end{bmatrix}.$$

With these notations, for each point correspondence $(\mathbf{x}_i, \mathbf{x}'_i)$ we have

$$d(\mathbf{x}'_i, \mathtt{F}\mathbf{x}_i) = |y'_i + c_i|,$$

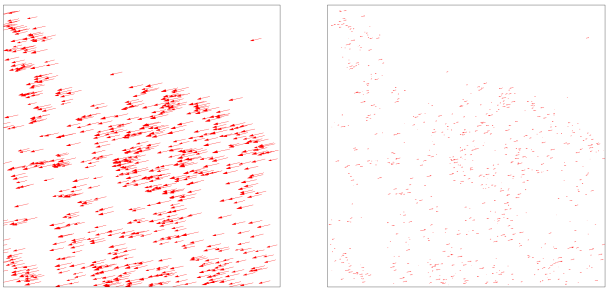

(a) (b)

Fig. 3. Error vectors for some keypoints on a 1000×1000 tile of a Pléiades image. (a) Error vectors before correction. (b) Error vectors after correcting the position of the second image by the optimal translation minimizing E'_{uv} (see equation 3).

where $\mathbf{x}'_i = (x'_i, y'_i, 1)^\top$. This error is invariant to any horizontal translation, thus the search for a translation minimizing function E'_{uv} as defined in equation 3 can be restricted to vertical translations only. With a vertical translation of parameter t, the function value becomes

$$E'_{uv}(\mathtt{T}) \approx \sum_{i=1}^{N} \mathrm{d}(\mathtt{T}\mathbf{x}'_i, \mathtt{F}\mathbf{x}_i) = \sum_{i=1}^{N} |y'_i + t + c_i|.$$

This sum is minimal when t is the median of $(-y'_i - c_i)_{i=1\ldots N}$. The relative pointing error can thus be minimized in a tile by applying a translation to one of the images. The translation is computed from a set of point correspondences with a closed-form expression.

4. EXPERIMENTAL RESULTS

The relative pointing error, as defined by equation 1, was measured on several Pléiades and a few WorldView-1 datasets. For each dataset the measurement was made with tiles sizes of 1000×1000 pixels (small) and $25\,000 \times 25\,000$ pixels (large). The tiles were located in the center of the reference image. The matches used to compute the relative pointing errors were obtained using SIFT [8]. Figure 3 shows the displacements that should be applied to the matching points of the second image to make them fit on the corresponding epipolar curves, before and after correction. Table 1 gives the measured values before and after correction, for both the tiles sizes (small and large). The correction was performed by computing the optimal translation in image space as described in section 3.3. The results show that, on average, for tiles of size 1000×1000, the relative pointing error is reduced by a factor 10 and is always smaller than half a pixel. On the contrary, for large tiles of size $25\,000 \times 25\,000$, the error is reduced on average by a factor 2, but the residual error may

Dataset	Alt. range width (m)	error small	resid. small	error large	resid. large
calanques	182	0.61	0.14	0.58	0.41
cannes	151	4.33	0.12	3.83	0.36
giza	57	0.63	0.09	0.39	0.40
lenclio	55	1.88	0.12	1.17	0.44
mera	1097	8.47	0.29	8.13	0.38
mercedes_1	19	2.01	0.15	2.07	0.31
mercedes_2	21	2.18	0.13	2.14	0.18
mont_blanc_1	466	2.23	0.15	2.13	1.35
mont_blanc_2	1159	3.25	0.21	3.05	1.27
montevideo	18	0.16	0.09	0.22	0.15
new_york	40	0.17	0.10	0.46	0.73
ossoue	540	1.02	0.36	0.80	0.43
reunion_1	79	1.13	0.10	3.34	2.49
reunion_3	72	0.99	0.10	1.07	0.17
reunion_4	28	0.80	0.12	0.77	0.21
reunion_5	349	0.72	0.13	0.67	0.19
spitsberg	610	1.16	0.27	1.12	4.58
toulouse	4	0.92	0.14	0.66	0.29
ubaye	220	0.27	0.17	0.31	0.36
ambedkar⋆	9	2.55	0.16		
charbagh⋆	16	2.35	0.48		
mean	–	1.80	0.17	1.57	0.7

Table 1. Pointing error values before and after correction (*residual*), for two tile sizes: *small* is 1000×1000 pixels and *large* is $25\,000 \times 25\,000$. On average, the proposed algorithm allows to reduce the error by a factor 10 on the small tiles, and a factor 2 on the large tiles. Thus the correction is used only for small tiles. Datasets marked with an asterisk ($\star$) are from Worldview-1. The others are from Pléiades 1A and 1B.

still be greater than 1 pixel, and in some cases the correction increases the error. There are two explanations for that:

- the pointing error is not well approximated by a translation in image space for such large tiles,
- the epipolar geometry is not well approximated by an affine fundamental matrix [9].

The energy defined in equation 2 was used for these large tiles, leading to an almost null rotation and almost the same residual errors. Nevertheless, this study shows that for stereo reconstruction purposes, which require only small tiles, the pointing error correction is satisfactory.

5. CONCLUSION

We presented a method to automatically correct the relative error that exists between the calibration data associated to two views of any Pléiades stereo dataset. This method reduces the relative error by a factor 10, lowering it under 0.2 pixels, thus allowing a very precise stereo-rectification. This pointing error correction method is implemented in the Satellite Stereo Pipeline (s2p), which can be tested online [10]. It is an automatic pipeline for computing digital elevation models and 3D points clouds from high resolution stereo and tri-stereo datasets. Figure 4 shows some of its results.

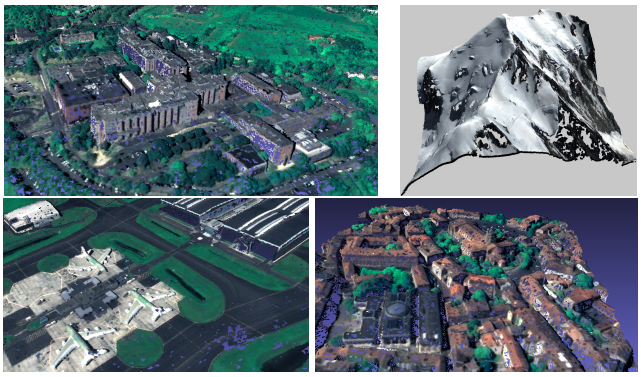

Fig. 4. These 3D point clouds were automatically generated from Pléiades tri-stereo datasets, without any manual interaction. The s2p pipeline is available online through a web interface [10].

6. REFERENCES

[1] H.B. Hanley, T. Yamakawa, and C.S. Fraser, "Sensor orientation for high-resolution satellite imagery," *International Archives of Photogrammetry Remote Sensing and Spatial Information Sciences*, vol. 34, no. 1, pp. 69–75, 2002.

[2] C.S. Fraser and H.B. Hanley, "Bias compensation in rational functions for ikonos satellite imagery," *Photogrammetric Engineering and Remote Sensing*, vol. 69, no. 1, pp. 53–57, 2003.

[3] J. Grodecki and G. Dial, "Block adjustment of high-resolution satellite images described by rational polynomials," *Photogrammetric Engineering and Remote Sensing*, vol. 69, no. 1, pp. 59–68, 2003.

[4] C.S. Fraser and H.B. Hanley, "Bias-compensated rpcs for sensor orientation of high-resolution satellite imagery," *Photogrammetric Engineering and Remote Sensing*, vol. 71, no. 8, pp. 909–915, 2005.

[5] E.P. Baltsavias and D. Stallmann, "Metric information extraction from spot images and the role of polynomial mapping functions," *International Archives of Photogrammetry and Remote Sensing*, vol. 29, pp. 358–364, 1992.

[6] I. Dowman and J.T. Dolloff, "An evaluation of rational functions for photogrammetric restitution," *International Archives of Photogrammetry and Remote Sensing*, vol. 33, pp. 254–266, 2000.

[7] C.V. Tao and Y. Hu, "A comprehensive study of the rational function model for photogrammetric processing," *Photogrammetric Engineering and Remote Sensing*, vol. 67, no. 12, pp. 1347–1357, 2001.

[8] D.G. Lowe, "Distinctive image features from Scale-Invariant keypoints," *Int. J. Comput. Vision*, vol. 60, 2004.

[9] C. de Franchis, E. Meinhardt-Llopis, J. Michel, J.-M. Morel, and G. Facciolo, "On stereo-rectification of pushbroom images," in *Image Processing (ICIP), 2014 21th IEEE International Conference on*, Oct 2014.

[10] C. de Franchis, G. Facciolo, and E. Meinhardt-Llopis, "s2p IPOL workshop," `http://dev.ipol.im/~carlo/s2p_igarss_2014/`, 2014.